Supporting Information

Boosting Li-S Redox Chemistry by Plasmonic Effect of MXene

Yu Liu, Xingyu Wang, Xiangyu Meng, Zhiyu Wang*

Experimental Section

Synthesis of $Ti_3C_2T_x$ MXene. The MXene was synthesized by etching the $Ti_3C_2T_x$ MAX phase.[S1] First, 13.2 g LiF and 5 g Ti_3AlC_2 MAX were added to 200 mL of 6 M hydrochloric acid and fully stirred. Second, the mixed solution was stirred continuously for 72 h at 45 °C. Thirdly, the MXene aqueous solution was harvested by several centrifugation-rinsing cycles with deionized (DI) water, followed by ultrasonic and centrifugation treatment. Finally, the obtained colloidal solution was frozen-dried to obtain MXene powder.

Synthesis of MXene@CC. For the preparation of MXene@CC, a suspension was made by dispersing $Ti_3C_2T_x$ MXene (4 mg) in a water/ethanol mixture (v/v = 1:1, 0.98 mL) with 5 wt.% Nafion (0.02 mL). This suspension was drop-cast onto carbon cloth (CC), followed by drying. The detail have been provided in the Experimental section in the revised Supporting Information, highlighted in yellow.

Material Characterization. The morphology of the samples was characterized by transmission electron microscopy (TEM, G2 F30 S-Twin). The infrared thermography of the electrodes was taken by a thermal infrared camera (FLIR, C5). The localized surface plasmon resonance (LSPR) of MXene was probed by a UV-vis spectrometer (PerkinElmer Lambda 750). X-ray photoelectron spectra (XPS) were measured on a Shimaduzu AXIS SUPRA+ spectrometer.

Femtosecond transient absorption spectroscopy of MXene. Time-resolved transient absorption measurements were performed using femtosecond laser pulses generated by

a Ti: sapphire laser system (Coherent Vitesse and Coherent Legend Elite He+ USP-1K-III; central wavelength ~800 nm, pulse duration ~35 fs, pulse energy ~7 mJ, repetition rate 1 kHz). A portion of the fundamental beam was directed into an optical parametric amplifier (OPA, Light Conversion: TOPAS+UV/VIS), producing tunable pump pulses spanning 240–2400 nm. A low-energy fraction of the fundamental pulse (1–2 μJ per pulse) was focused onto a sapphire plate to generate a white-light supercontinuum (450–750 nm), which served as the probe. Both pump and probe beams were spatially and temporally overlapped on the sample. Temporal delays were introduced using a motorized optical delay stage (ALS10045-S-M-10-MT-LT45AS-CM, Aerotech), with step sizes of 25 fs within the 0–1.5 ps time window. A synchronized chopper modulated the pump beam at 500 Hz, while a neutral-density filter was employed to control the excitation fluence. The polarization of the pump beam was adjusted using a half-wave plate ($\lambda/2$). The probe beam was directed into a fibre-coupled spectrometer (AvaSpec-ULS2048CL-EVO, Avantes) to record transient transmission changes ($\Delta T/T$). A polarizer positioned before the spectrometer inlet suppressed scattered pump light.

Assembly and test of three-electrode cells. The working electrode was prepared by dispersing 4 mg of $Ti_3C_2T_x$ into 0.98 mL of a water/ethanol mixture (v/v = 1:1), followed by the addition of 0.02 mL of a 5 wt% Nafion solution. The suspension was sonicated for 1 h to achieve a uniform dispersion. Then, 10 μL of the resulting slurry was drop-cast onto the surface of a glassy carbon electrode (diameter = 5 mm) and allowed to dry under ambient conditions. Electrochemical measurements were conducted in a square quartz cuvette using a three-electrode configuration. The working electrode consisted of a $Ti_3C_2T_x$-coated, L-shaped glassy carbon electrode (d = 5 mm). A graphite rod acts as the counter electrode, and Li metal foil as the reference. The LS-009 electrolyte comprises 1 M lithium bis(trifluoromethanesulfonyl)imide (LiTFSI) and 1 wt% lithium nitrate ($LiNO_3$) dissolved in a 1:1 volume ratio mixture of 1,3-dioxolane (DOL) and dimethoxyethane (DME). During testing, 0.05 M Li_2S_6 was introduced as the redox-active species. To mitigate undesirable redox interactions

between the reference electrode and Li_2S_6, the lithium metal reference was immersed in a salt bridge filled with the above electrolyte. The linear sweep voltammetry (LSV) and galvanostatic charge-discharge curves were performed using an electrochemical workstation (IVIUM).

Fabrication of the S/MXene cathode. The cathode was prepared via a melt-infusion method using a porous carbon cloth current collector modified with $Ti_3C_2T_x$ MXene. Specifically, 40 mg of sublimed sulfur was dissolved in 2 mL of carbon disulfide (CS_2) to form a uniform solution, which was then drop-cast onto the MXene@CC substrate. After natural drying in a fume hood, the electrode was thermally treated at 155 °C for 15 h in an argon-filled autoclave to obtain the final S/MXene@CC composite. The sulfur loading was approximately 2 mg cm^{-2}.

Assembly and testing of Li-S coin cells. Coin cells were assembled using modified CR2016-type casings featuring a transparent optical window (diameter: 6 mm) on the cathode side. A quartz coverslip (φ = 13 mm) was affixed over the window using UV-curable adhesive to hermetically seal the cell, preventing exposure of the electrolyte and active materials to ambient air while enabling direct light irradiation onto the electrode surface. Cell assembly was carried out in an argon-filled glovebox, with oxygen and moisture levels strictly controlled below 0.1 ppm. The LS-009 served as the electrolyte. During assembly, a stainless steel mesh was placed between the cathode and the optical window to enhance heat dissipation and electronic conductivity on the cathode side. The cell was sealed and rested for 6 h to ensure thorough electrolyte wetting of the electrodes before electrochemical tests. The cyclic voltammetry (CV) tests were performed from 1.7 to 2.8 V at a scan rate of 0.1 mV s^{-1} using a Vertex.C.EIS electrochemical workstation (IVIUM). The electrochemical impedance spectroscopy (EIS) tests were conducted in the frequency range of 100 kHz to 0.01Hz with an amplitude of 5 mV by the same workstation. The rate and cycling performance were carried out on a LAND CT2001A battery tester.

Assembly and testing of transparent cells. Transparent full batteries were assembled using ITO transparent conductive films as both the current collector and packaging material. A thin layer of gold was deposited on the ITO surface by magnetron sputtering to enhance the interfacial affinity between the ITO substrate and the electrode slurry. The cathode was made by thermal treatment of sulfur and $Ti_3C_2T_x$ MXene at a mass ratio of 8:2 in an Ar-filled reactor at 155 °C for 15 h. The obtained composite was then mixed with conductive carbon and PVDF binder at a mass ratio of 8:1:1 in N-methyl-2-pyrrolidone (NMP). The formed slurry was uniformly coated onto the gold-coated ITO film and vacuum-dried for 12 h to completely remove the NMP solvent. The sulfur loading was approximately 1.5 mg cm^{-2}. The anode was fabricated by mixing Si nanoparticles, $Ti_3C_2T_x$ MXene and sodium carboxymethyl cellulose (CMC) at a mass ratio of 7:2:1 in deionized water. The formed slurry was uniformly coated onto the gold-coated ITO film and vacuum-dried for 6 h to completely remove the water. The Si loading was 1.5 mg cm^{-2}. Prior to assembling the transparent battery, the anode was deeply prelithiated by intimate contact the above Si anode with a Li metal foil, between which the interface was thoroughly wetted with LS-009 electrolyte. Driven by the potential difference, Li^+ spontaneously intercalated into the Si, converting it into a fully lithiated state after 10 h.

Calculation of the extinction coefficient of MXene. The extinction coefficient ε was calculated by performing a linear fit of the absorbance at 780 nm in the UV-Vis absorption spectra of MXene aqueous solutions with varying concentrations based on the Lambert-Beer law:[1]

$$A(\lambda) = \varepsilon LC \quad (1)$$

where A is the absorbance at a wavelength of λ, L is the optical path length and C is the concentration of MXene aqueous solutions.

Calculation of photothermal conversion efficiency of MXene. The photothermal conversion efficiency was calculated as the ratio of the energy converted from light to heat to the total received optical energy. The energy balance of the entire system adheres

to the following equation:[S2]

$$\sum_i m_i C_{p,i} \frac{dT}{dt} = Q_{MXene} + Q_{Dis} - Q_{surr} \quad (2)$$

where m and C_p are the mass and heat capacity of water, T is the temperature of MXene aqueous solutions, Q_{MXene} is the optical energy captured by MXene, Q_{Dis} the baseline energy of the sample cell and Q_{surr} is the heat energy dissipated from the system to the surrounding environment. Q_{MXene}, Q_{Dis} and Q_{surr} are determined by the following equations:

$$Q_{MXene} = I(1 - 10^{-A_\lambda})\eta \quad (3)$$

$$Q_{Dis} = hS(T_{max,water} - T_{surr,water}) \quad (4)$$

$$Q_{Dis} = hS(T - T_{surr}) \quad (5)$$

where I is the energy of NIR light, A_λ is the absorbance of MXene at λ = 808 nm, η is the photothermal conversion efficiency of MXene, T and T_{surr} are the temperatures of the system surface and the surrounding environment, $T_{max,water}$ and $T_{surr,water}$ are the temperature of pure water after being exposed to the NIR light and under ambient conditions, h is the heat transfer coefficient and S is the surface area of the heat transfer. The hS is calculated according to the following equations:

$$\theta = \frac{T - T_{surr}}{T_{max} - T_{surr}} \quad (6)$$

$$\tau_s = \frac{\sum_i m_i C_{p,i}}{hS} \quad (7)$$

where θ is defined as the driving force for heat exchange and τ_s is the time constant of the sample system.

At the cooling period of MXene aqueous solution, no additional energy is input, that is

$$Q_{MXene} + Q_{Dis} = 0 \quad (8)$$

The heat transfer time constant τ_s can be determined from the cooling curve as follows:

$$dt = -\tau_s \frac{d\theta}{\theta} \quad (9)$$

and integrating gives the expression

$$t = -\tau_s \ln\theta \tag{10}$$

Therefore, the time constant of heat transfer from the system was determined:

$$\eta = \frac{hS(T_{max}-T_{surr})-Q_{Dis}}{I(1-10^{-A_\lambda})} \tag{11}$$

Calculation of the reaction activation energy difference (ΔE_a). The relative activation energies of the redox process with or w/o near-infrared illumination could be calculated according to equation:[S3]

$$E_a = E_a^0 + \alpha zF\varphi_{cathode}(Ox|Res)_{IR} \tag{12}$$

where E_a is the activation energy of the redox process, E_a^0 is the intrinsic activation energy, α is the symmetry coefficient, z is the number of charge transfer, F is the Faraday's constant, $\varphi_{cathode}(Ox|Res)_{IR}$ is the irreversible potential during cycling.

The Tafel curve calculation formula:

$$\eta_{vathode} = \frac{RT}{\alpha zF} lnj_0 - \frac{RT}{\alpha zF} lnj_{cathode} \tag{13}$$

Where $\eta_{vathode}$ is the overpotential of the cathode, j_0 is the exchange current density, $j_{cathode}$ is the current of the cathode. The equation can be written in a more concise form:

$$\eta_{vathode} = a + blnj_{cathode} \tag{14}$$

$$b = a - \frac{RT}{\alpha zF} \tag{15}$$

Where a is the intercept of the Tafel curve, b is the slope of the Tafel curve. Therefore, equation (15) can be written in a more concise form:

$$E_a = E_a^0 - \frac{RT}{b}\varphi_{cathode}(Ox|Res)_{IR} \tag{16}$$

The difference in activation energy could be calculated by subtracting the activation energy of the electrode in the dark from that under illumination.

$$\Delta E_a = E_{a2} - E_{a1} = \frac{RT}{b_1}\varphi_{cathode}(Ox|Res)_{IR1} - \frac{RT}{b_2}\varphi_{cathode}(Ox|Res)_{IR2} \tag{17}$$

References

[S1] Y. Liu, X. Meng, Z. Wang, J. Qiu, Sci. Adv., 2022, eabl8390

[S2] H. Lin, S. Gao, C. Dai, Y. Chen and J. Shi, J. Am. Chem. Soc., 2017, 139, 16235.

[S3] W. Hua, H. Li, C. Pei, J. Xia, Y. Sun, C. Zhang, W. Lv, Y. Tao, Y. Jiao, B. Zhang, S. Z. Qiao, Y. Wan and Q. H. Yang, Adv. Mater., 2021, 33, 2101006.

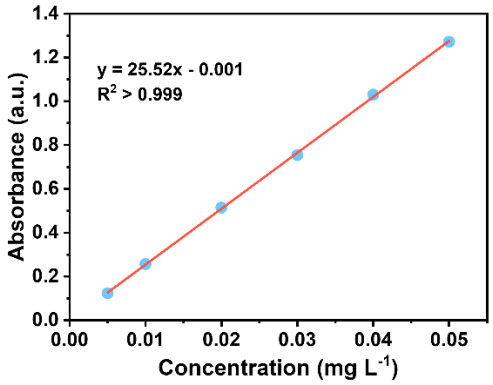

Figure S1. The linear fitting result of MXene colloid concentration with absorbance in UV-Vis-NIR absorption spectra.

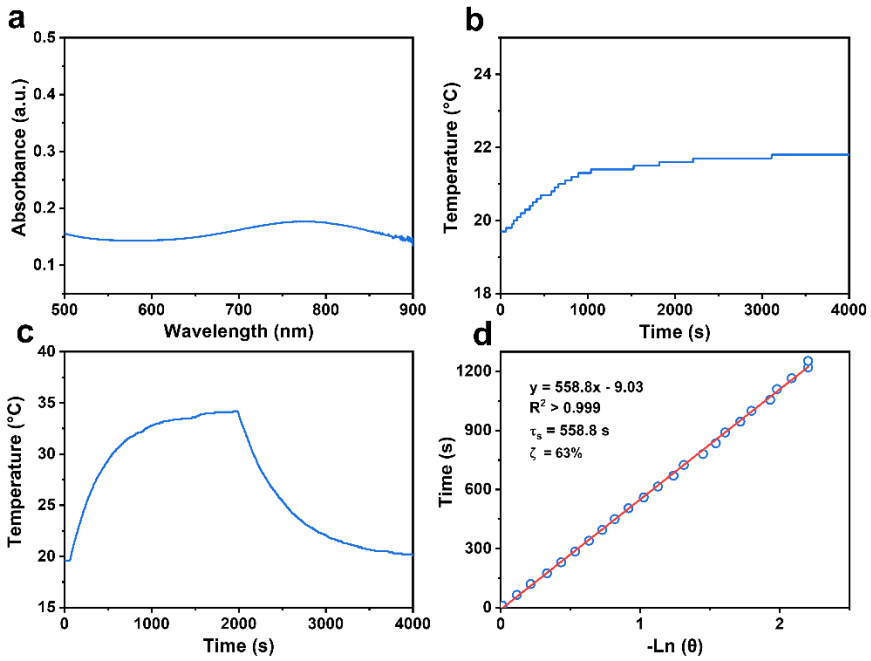

Figure S2. Calculation of photothermal conversion efficiency. (a) UV-Vis-NIR spectrum of MXene colloid. Photothermal effect under NIR light power of 1.35 W cm^{-2} for (b) pure water, (c) MXene colloid, and (d) the linear fitting result.

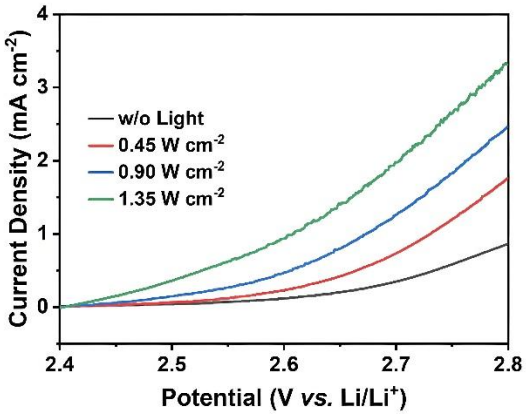

Figure S3. LSV curves of Li_2S_6 oxidation on $Ti_3C_2T_x$ MXene in a three-electrode system at various NIR light power densities.

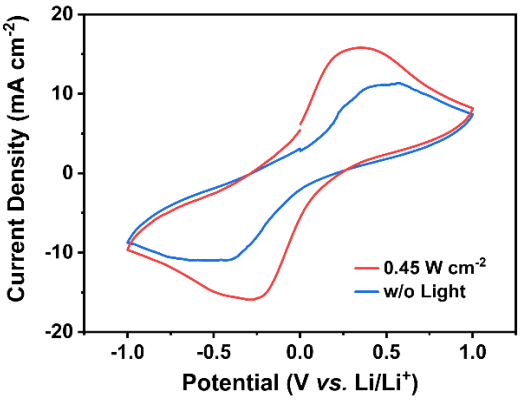

Figure S4. CV curves of symmetric cells utilizing Li_2S_6 as the active material at a scan rate of 10 mV s^{-1} under the dark conditions or NIR light power of 0.45 W cm^{-2}.

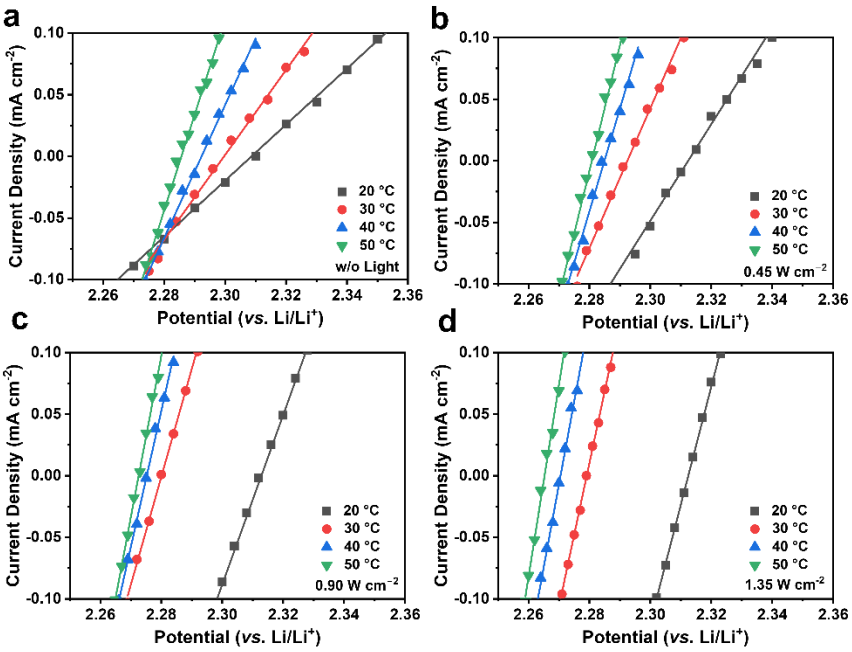

Figure S5. I-U curves of Li_2S_6 reactions on $Ti_3C_2T_x$ MXene near the balanced potential at different temperatures (a) under the dark conditions, and different NIR light power of (b) 0.45 W cm^{-2}, (c) 0.90 W cm^{-2} and (d) 1.35 W cm^{-2}.

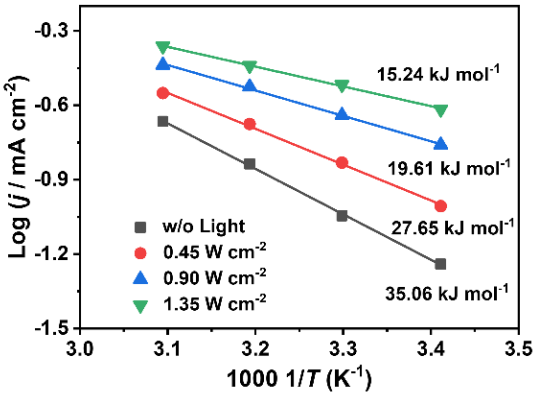

Figure S6. Calculation of activation energy of Li_2S_6 reduction on $Ti_3C_2T_x$ MXene under the dark conditions, and different NIR light power.

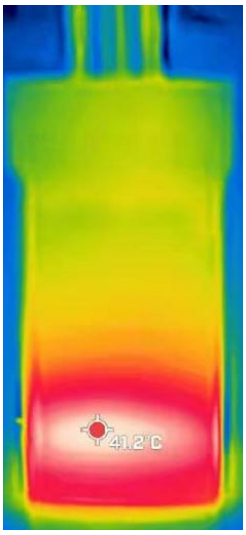

Figure S7. Infrared thermography of $Ti_3C_2T_x$ MXene electrode under a NIR light power of 1.35 W cm^{-2}.

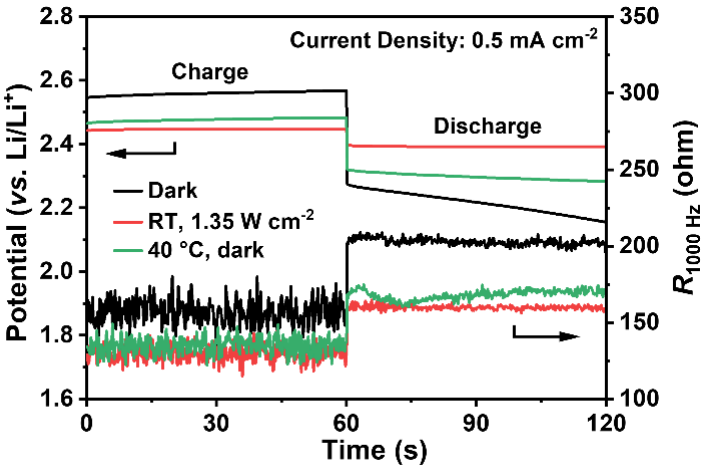

Figure S8. The impedance at a frequency of 1000 Hz during the galvanostatic charge-discharge process at dark conditions, NIR light power of 1.35 W cm^{-2}, and heating the electrolyte to 40 ºC without light irradiation.

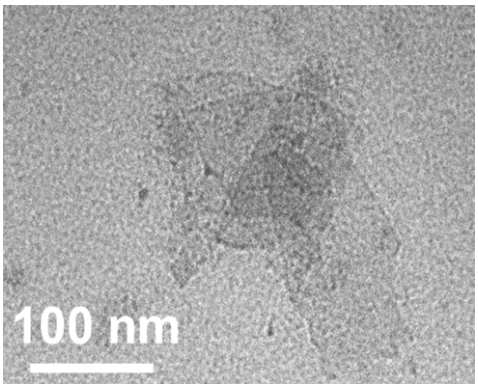

Figure S9. TEM image of MXene after cycling in the Li_2S_6-containing electrolyte.

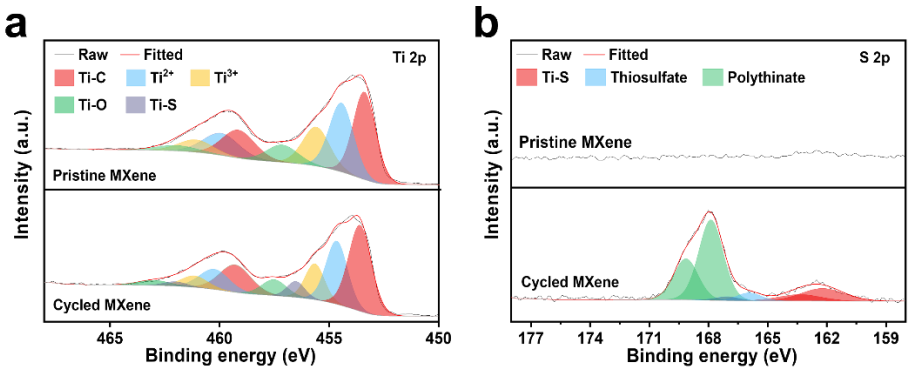

Figure S10. (a) Ti 2*p* XPS and (b) S 2*p* XPS spectra of MXene before and after cycling in Li_2S_6-containing electrolyte.

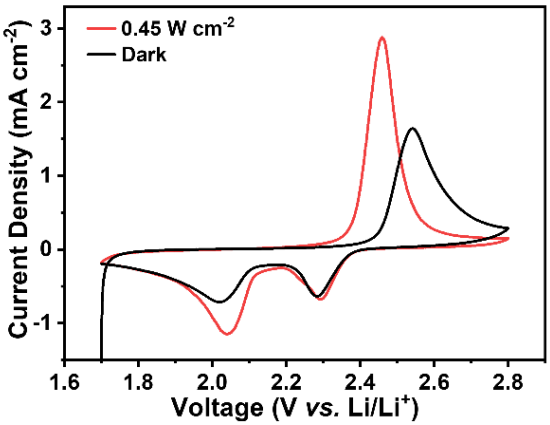

Figure S11. The CV curves of Li||S/MXene cells under the dark conditions or NIR light power of 0.45 W cm^{-2}.

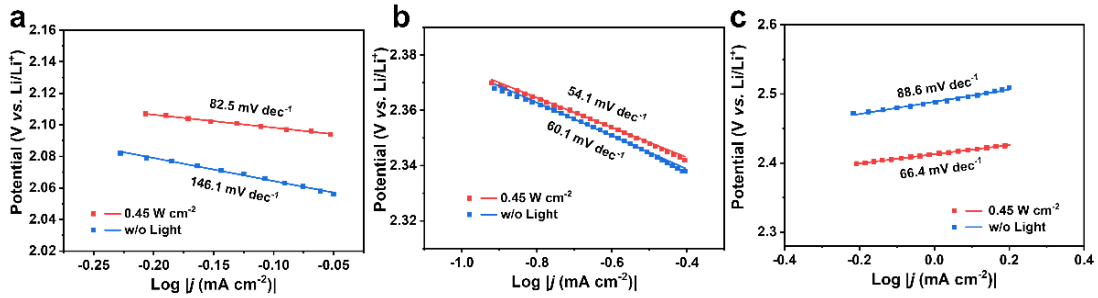

Figure S12. Tafel slopes for different redox processes in Li||S/MXene cells under the dark conditions or NIR light power of 0.45 W cm^{-2}.

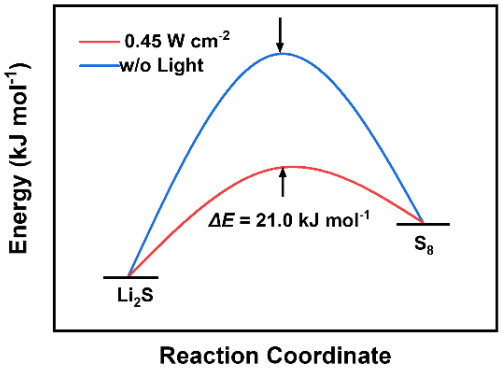

Figure S13. The relative activation energies for charge process of Li||S/MXene cells under the dark conditions and NIR irradiation.

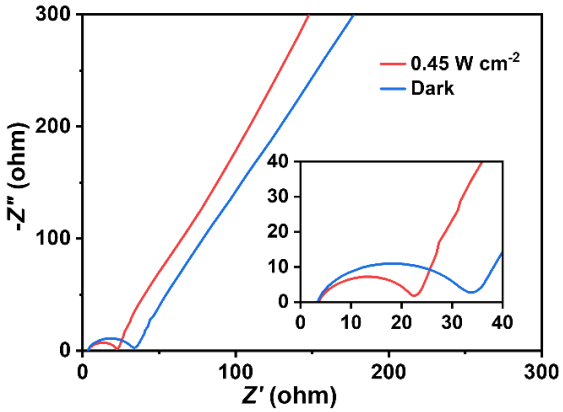

Figure S14. EIS measurements of in Li||S/MXene cells before the first cycle under the dark conditions or NIR light power of 0.45 W cm^{-2}.

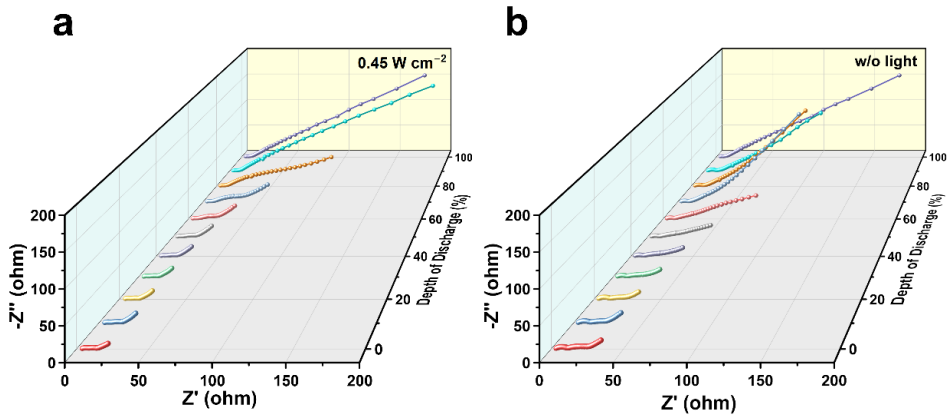

Figure S15. EIS measurements of in Li||S/MXene cells during the discharge process (a) under the dark conditions or (b) NIR light power of 0.45 W cm^{-2}.

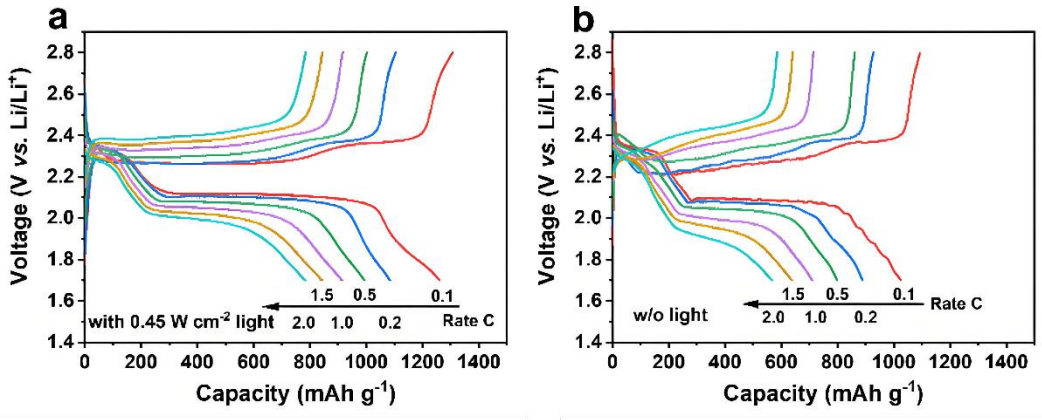

Figure S16. Charge and discharge curves of Li||S/MXene cells at various current rates (a) under NIR irradiation or (b) in the dark.

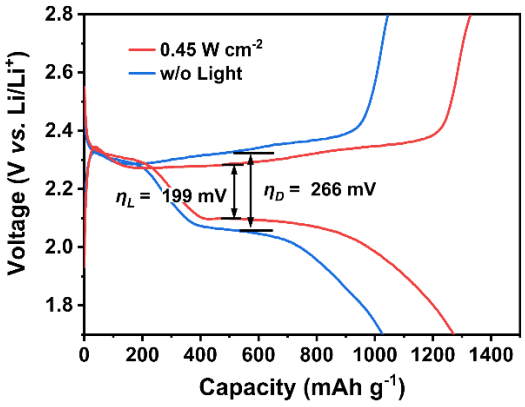

Figure S17. Charge-discharge profiles of Li||MXene/S cells under the dark conditions or NIR light power of 0.45 W cm^{-2} at 0.1 C.

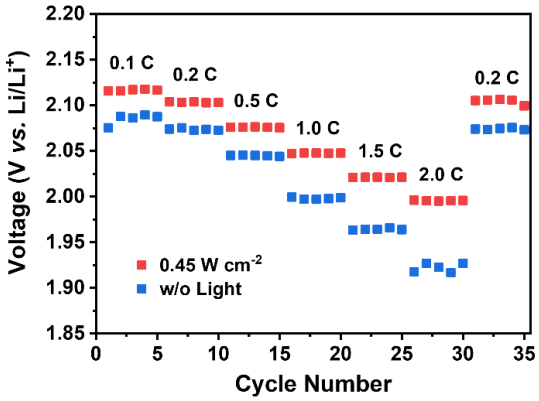

Figure S18. Potential change of Li||MXene/S cells under the dark conditions and NIR irradiation at a light power of 0.45 W cm^{-2}.

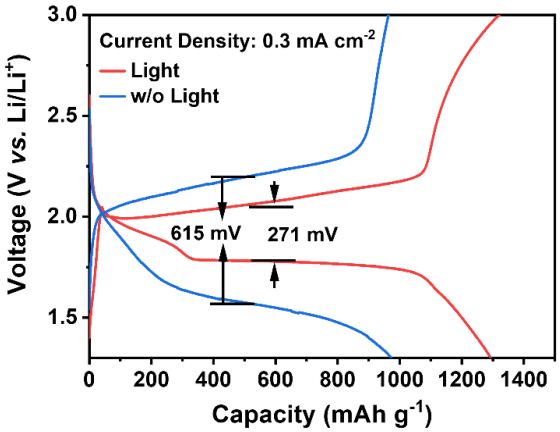

Figure S19. Charge and discharge curves of a transparent full battery with and without one-sun irradiation at a current density of 0.3 mA cm^{-2}.

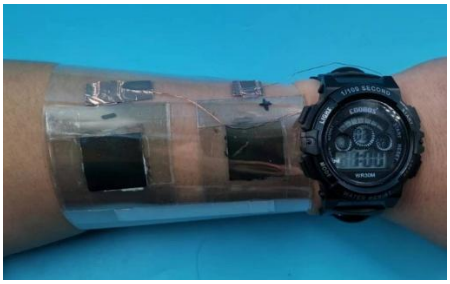

Figure S20. Digital image of a transparent cells under bending state for powering an electronic watch.